Journal of Materials Science: Materials in Medicine (2018) 29:44
https://doi.org/10.1007/s10856-018-6050-8

BIOCOMPATIBILITY STUDIES

Original Research

Investigation on the *in vitro* cytocompatibility of Mg-Zn-Y-Nd-Zr alloys as degradable orthopaedic implant materials

Xiaozhe Song[1] · Lei Chang[1] · Jun Wang[1] · Shijie Zhu[1] · Liguo Wang[1] · Kun Feng[2] · Yage Luo[2] · Shaokang Guan[1]

Received: 22 January 2018 / Accepted: 16 March 2018 / Published online: 30 March 2018

Abstract

Mg-Zn-Y-Nd-Zr alloy has been developed as a new type of biodegradable orthopaedic implant material by the authors' research group with its excellent mechanical properties and controllable degradation rate. In this study, the cytocompatibility of Mg-Zn-Y-Nd-Zr alloy was systematically evaluated through *in vitro* cell culture method. MTT assay was applied to evaluate the cytotoxicity of Mg-Zn-Y-Nd-Zr alloy and no toxic effect was observed on L929 and MC3T3-E1 cells followed the protocol of ISO 10993 standard. Considering the potential ion accumulation in the bony environment, this study further investigated the cytotoxic effect of accumulated metallic ions during the alloy degradation by extending the extract preparation time. When the extract preparation time was prolonged to 1440 h, the accumulated metallic ions leaded to severe cell apoptosis, of which the combined ion concentration was determined as 39.5–65.8 μM of Mg^{2+}, 3.5–5.9 μM of Zn^{2+}, 0.44–0.74 μM of Y^{3+}, 0.3–0.52 μM of Nd^{3+} and 0.11–0.18 μM of Zr^{4+} for L929, and 65.8–92.2 μM of Mg^{2+}, 5.9–8.3 μM of Zn^{2+}, 0.74–1.04 μM of Y^{3+}, 0.52–0.73 μM of Nd^{3+} and 0.18–0.25 μM of Zr^{4+} for MC3T3-E1 cells. Besides the cell viability assessment, high expression of ALP activity and calcified nodules implied that metal elements in Mg-Zn-Y-Nd-Zr alloys can promote the osteogenic differentiation. Hence, excellent cytocompatibility has equipped Mg-Zn-Y-Nd-Zr alloy as a promising candidate for orthopaedic implant application, which can remarkably guide the magnesium-based alloy design and provide scientific evidence for clinical practice in future.

1 Introduction

Magnesium and its alloys are promising candidates to be used as orthopaedic implant materials due to the unique properties, such as similar density and elastic modulus to natural bone, biodegradability and good mechanical properties [1, 2]. Magnesium is naturally found in bone and essential to human metabolism [1]. However, excessive degradation of magnesium and its alloys results in steep increase of pH value, metallic ion release, loss of mechanical strength and subcutaneous gas pockets formation during service period in human body [3], and eventually leads to the implant failure. Alloying of magnesium is an effective approach to enhance the corrosion resistance and thus improves the clinical application prospect [4]. Rosalbino [5] proved an improvement of the corrosion resistance of Mg-Zn-Mn alloys with increasing Zn and Mn content attributed to the enhanced protective capabilities of $Mg(OH)_2$ surface film by the alloying elements. Tie [6] investigated the *in vivo* biocompatibility of Mg-Sr alloy as the femoral fracture fixation device in New Zealand white rabbits. The corrosion rate was measured to be 0.55 ± 0.03 mm y^{-1} which satisfied the bone implant requirements. Chou [7] proposed that the increase of Y content helped to improve the corrosion resistance of Mg-Y-Ca-Zr alloy and introduced it as orthopaedic and craniofacial implant biomaterials.

As biodegradable biomaterials, alloy elements in the metal implants should not only decrease the corrosion rate and improve the mechanical strength but also be biocompatible, as they will enter the body in ionic form eventually instead of residing inside the metal implant with regards to permanent implants, so the biocompatibility of

✉ Lei Chang
changlei@zzu.edu.cn

✉ Jun Wang
wangj@zzu.edu.cn

✉ Shaokang Guan
skguan@zzu.edu.cn

[1] School of Materials Science and Engineering, Zhengzhou University, Zhengzhou 450002, China

[2] Orthopaedic Institute of Henan Province, Luoyang 471000, China

implants should be considered thoroughly [8]. Mg-Zn-Y-Nd-Zr alloy was developed by the authors' group and has been patented in China (patent No. CN103526091A). As compared with as-extruded WE43, yield strength and corrosion resistance of Mg-Zn-Y-Nd-Zr increased by 18 and 70%, respectively, showing great potential for application in bone fixation. The addition of Y and Nd elements in magnesium alloys was proved to be less cytotoxic and favorably biocompatible in comparison with other rare earth elements in previous studies [9]. Willbold [10] showed the addition of low rare earth elements (Lanthanum, Neodymium, Cerium) in magnesium alloys caused no systematic or local cytotoxicological effects clinically and histologically. The neodymium-containing alloy exhibited the lowest corrosion rates while the lanthanum- and cerium-containing alloys degraded at comparable rates. Zhang [11] suggested Y^{3+} promoted the proliferation of osteoblast cells at tested concentrations and effects of yttrium ion on mineralization function could be switched from down-regulation to up-regulation depending on its concentrations and culture time. Besides, Y element has already been used in medical field [12]. Zirconium (Zr) is added to magnesium alloys mainly as grain refiner. Saha [3] proved smaller grain size not only contributed to the mechanical strength improvement and bioactivity, but also enhanced osteoblast cell activity and proliferation due to higher grain boundary area per unit area, thus suggesting the design of novel degradable Mg alloys with suitable alloying elements implemented in conjunction with Zr.

Although the alloying elements are relatively low-toxic as reported, the biological safety and functionality of Mg-Zn-Y-Nd-Zr alloy have to be explored thoroughly before the clinical usage. This study proposes the Mg-Zn-Y-Nd-Zr alloy as the potential candidate for orthopaedic application with improved corrosion resistance, and focuses on the *in vitro* cytocompatibility of Mg-Zn-Y-Nd-Zr alloy. Experiments were distinguishingly designed to emphasize the coupling effects of metallic ions (Mg^{2+}, Zn^{2+}, Y^{3+}, Nd^{3+} and Zr^{4+}) released during the degradation process and the cytotoxic level of combined metallic ions was revealed, which may significantly help the material design of biodegradable magnesium-based alloys.

2 Materials and methods

2.1 Materials

As-extruded Mg-Zn-Y-Nd-Zr alloys were used in this study. The cylindrical samples of dimensions 9.6 mm × 40 mm and 9.6 mm × 1.5 mm (diameter × thickness) were cut from as-extruded rods for the extract preparation and cell adhesion tests, respectively. The surface of samples was successively polished up to 800 grit SiC paper, followed by ultrasonically cleaning in absolute ethanol for 10 min and then air-dried. Prior to the *in vitro* tests, ultraviolet (UV) was used for sample sterilization. In this study, as-extruded Mg-Zn-Y-Nd alloys were utilized for comparison purpose, which also followed the preparation protocol as described above.

2.2 Microstructural analysis

The surface of samples was polished and etched with a mixture of 1.5 g picric acid, 10 ml acetic acid, 25 ml ethanol and 20 ml deionized water (purchased from Sigma Aldrich, USA). All etched samples were further rinsed in ethanol and analyzed with optical microscope (Leica, DM4000M, Germany). Grain size was measured according to the method described in ASTM E112:2004.

2.3 Electrochemical tests

Electrochemical workstation (RST 5200, China) was utilized to investigate the corrosion properties of Mg-Zn-Y-Nd-Zr alloys. Samples were embedded into epoxy resin with only one side of 0.73 mm^2 exposed to simulated body fluid (SBF) [13]. Tests were performed at 37 °C and scan rate was set to 0.5 mV/s.

2.4 Extract preparation

The extracts of both Mg-Zn-Y-Nd-Zr and Mg-Zn-Y-Nd samples were prepared according to ISO 10993-12: 2004 [14]. Samples were immersed into culture medium for 24 h under cell culture conditions (5% CO_2, 95% humidity, 37 °C), with a fixed ratio of surface areas to medium volume of 1.25 cm^2/ml. The extracts were collected to evaluate cytotoxicity and cell differentiation.

2.5 Cytotoxicity test

Murine fibroblast cells (L929) and murine calvarial pre-osteoblasts (MC3T3-E1) were obtained from Shanghai Institutes for Biological Sciences (Chinese Academy of Sciences, China). Both types of cells were cultured in alpha-minimal essential medium with no phenol red (α-MEM, Gibco, USA) supplemented with 5% fetal bovine serum (FBS, Gibco, USA) and 1% penicillin/streptomycin (P/S, Hyclone, USA) in order to avoid the interference of phenol red and high fetal bovine serum on the absorbance values. L929 and MC3T3-E1 were seeded in 96-well plates with a density of 4.0×10^3 cells/well, and pre-cultivated for 24 h. Subsequently, the supernatant was replaced by different concentrations of extracts varied from 20% to 100% diluted with culture media, and incubated for another 24 h.

An incubated medium without extracts was used as a blank control group, and 10% dimethyl sulfoxide (DMSO) without extracts was used as a cytotoxic reference group. The cell viability was tested using MTT assay (Solabio, China). The amount of formazan was quantified by measuring the absorbance using a microplate reader (Tecan Infinite F50, Austria) at a wavelength of 570 nm. According to ISO 10993-5:2009[15], a relative metabolic activity of less than 75% was regarded as cytotoxic.

2.6 Toxicity evaluation of accumulated metallic ions during Mg-Zn-Y-Nd-Zr degradation process

Accompanied by degradation of the Mg-alloy, the released amounts of Mg^{2+}, Zn^{2+}, Y^{3+}, Nd^{3+}, Zr^{4+} ions were cumulatively increased. Therefore, the immersion duration of extract preparation was prolonged to short term (48, 72, 120 and 240 h) and long term (1440 h) to investigate the toxicity of accumulated metallic ions. To avoid the decisive impact of the high pH value on cytotoxicity, it was adjusted to 7.4 using 1 M HCl. MTT assay was utilized to analyze the survival rates, and both of L929 and MC3T3-E1 cells were evaluated.

2.7 Cell adhesion

To analyze the direct cell adhesion on alloy surface, L929 and MC3T3-E1 cells were seeded on the sample surface in 24-well plates at a density of 1.5×10^4 and 9×10^3 cells/well, respectively. After 30 min incubation, 1 ml fresh medium was supplemented into each well, incubating for 5 h. Subsequently, culture medium was aspirated, and phosphate buffered saline (PBS, Hyclone, USA) was used to wash away the non-adherent cells on samples. Afterwards, Ethylene diamine tetraacetic acid-trypsin (EDTA-trypsin, Hyclone, USA) was added to digest adherent cells on samples. The trypsinized cells were rinsed into bottom of the well with 1 ml fresh medium and cells were observed under inverted phase contrast microscope (Nikon Eclipss Ts100, Japan). The adhesion rates were calculated according to the following formula: adhesion rate = number of adherent cells/ total number of seeded cells × 100%.

2.8 Cell differentiation

To examine the effect of concentration of metallic ions of Mg^{2+}, Zn^{2+}, Y^{3+}, Nd^{3+} and Zr^{4+} ions to osteogenic differentiation process, extracts of alloys were prepared according the protocol described in Section 4 with the adjustment of pH value to 7.4 and the culture medium was changed to Dulbecco's Modified Eagle Media: Nutrient Mixture F-12 (DMEM/F12, Hyclone, USA). In this test, primary bone marrow-derived mesenchymal stromal cells (BMSCs) were isolated from Sprague Dawley male rats and cultured in DMEM/F12 supplemented with 10% FBS (Gibco, USA) and 1%P/S (Hyclone, USA). The number < SYXK(Henan)2016-0002 > of the approval was provided by the committees of Zhengzhou University and Henan Province, China. When BMSCs covered about 80% of the bottom area of culture dish, osteogenic induce supplement (OIS) composed of 0.1 mol/L β-sodium glycerophosphate, 10^{-8} mol/L dexamethasone and 50 mol/L vitamin C was added into medium to induce osteogenic differentiation. Samples were divided into two groups: osteogenic medium (DMEM/F12 + 10%FBS + 1%P/S + OIS) and Mg-Zn-Y-Nd-Zr osteogenic medium (Mg-Zn-Y-Nd-Zr extracts + OIS).

2.8.1 Alkaline phosphatase (ALP) activity

Alkaline phosphatase (ALP) activity of cells in the sample extracts at day 9 was estimated according to the procedure used by Zhai [16] through an ALP assay kit (Nanjing Jiancheng Bioengineering Institute, China). Optical density of generated products was measured at 490 nm using the microplate reader (Tecan Infinite F50, Austria) and total cellular ALP activity was represented by the absorbance value.

2.8.2 Alizarin red staining (ARS)

Histochemical staining of calcified nodules was conducted using alizarin red staining agent to evaluate the osteogenic differentiation. At day 21, culture medium was discarded. Samples were thoroughly washed by PBS (Hyclone, USA) and fixed by the addition of 10% formaldehyde for 10 min before reacting with 0.1 g alizarin red (Solarbio, Beijing) added to 10 ml Tris-HCl buffer (pH = 8.32), and eventually incubated for 1 h at 37 °C.

2.9 Ion concentration analysis

Metallic ion concentrations of Mg^{2+}, Zn^{2+}, Y^{3+}, Nd^{3+} and Zr^{4+} in extracts and culture medium were quantified with an inductively coupled plasma atomic emission spectrometric (ICP-AES, 213DF0G ASDWE, Japan).

2.10 Statistical analysis

One-way ANOVA with Tukey post hoc test was used to determine any significant differences existed between the mean values of the experimental groups using Prism® version 6 (GraphPad, California). A difference between groups was considered to be significant indicated by * and † for $p < 0.001$ and $p < 0.05$, respectively. Cell viability test was performed in sixfold parallel measurement and the other

tests in fourfold parallel measurement. The mean values were calculated.

3 Results

3.1 Microstructure analysis and electrochemical measurement

Figure 1 demonstrated the grain structure of as-extruded Mg-Zn-Y-Nd-Zr samples. It can be observed that both of the samples exhibited the typical structure of equiaxial crystals. The granular second phase was dispersed inside the grains, and a small amount of second phase was uniformly distributed at the grain boundary. In contrast with Mg-Zn-Y-Nd, the average grain size of Mg-Zn-Y-Nd-Zr decreased from 9.5 to 1.3 μm (as shown in Fig. 1c which resulted from the grain refinement of the addition of Zr.

Electrochemical test was conducted to evaluate the *in vitro* corrosion properties of Mg-Zn-Y-Nd-Zr alloys. As summarized in Table 1, Mg-Zn-Y-Nd-Zr samples presented better corrosion resistance in SBF, with the corrosion current density (I_{corr}) decreased by 50% compared to Mg-Zn-Y-Nd samples. The reason may be that more grain boundaries in Mg-Zn-Y-Nd-Zr samples served as corrosion barrier, and then slowed down the general as well as localized corrosion rates [17].

3.2 Short-term cytotoxicity analysis

According to ISO 10993-5:2009 [15], cells and extracts should culture together for 24 h, and the cytotoxicity could be identified when cell viability is lower than 75%. To evaluate the short-term cytotoxicity, L929 and MC3T3-E1 cells were selected and MTT assay was utilized, of which the results were shown in Fig. 2. As for L929, the cell viability of all the Mg-Zn-Y-Nd-Zr groups was significantly higher than both control group and Mg-Zn-Y-Nd group, ranging from 100 to 125%, which indicated the excellent cytocompatibility. On the contrary, severe toxicity was observed for Mg-Zn-Y-Nd extracts in the concentrations of 60, 80 and 100%. In addition, cell proliferation of L929 seemed to be promoted in Mg-Zn-Y-Nd-Zr extracts. Similar phenomenon was observed when culturing with MC3T3-E1 cells (as shown in Fig. 3b). No cytotoxicity of all the Mg-Zn-Y-Nd-Zr groups was detected, and cells tended to multiply more significantly in Mg-Zn-Y-Nd-Zr extracts, of which the cell viability reached up to 120%. The viability differences between Mg-Zn-Y-Nd-Zr and

Table 1 Results of the potentiodynamic polarization measurements. (E_{corr}: open circuit potential, I_{corr}: corrosion current density)

Sample	E_{corr} (V)	I_{corr} (A·cm^{-2})
Mg-Zn-Y-Nd	−1.79	2.13×10^{-4}
Mg-Zn-Y-Nd-Zr	−1.68	1.06×10^{-4}

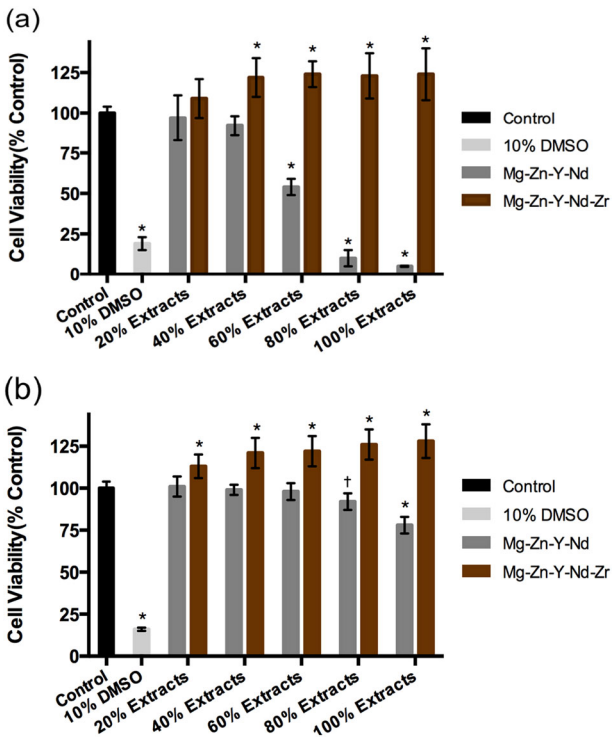

Fig. 2 Cell viabilities of **a** L929 and **b** MC3T3-E1 cultured in extracts for 24 h. *$p < 0.001$ and †$p < 0.05$ compared to the control group

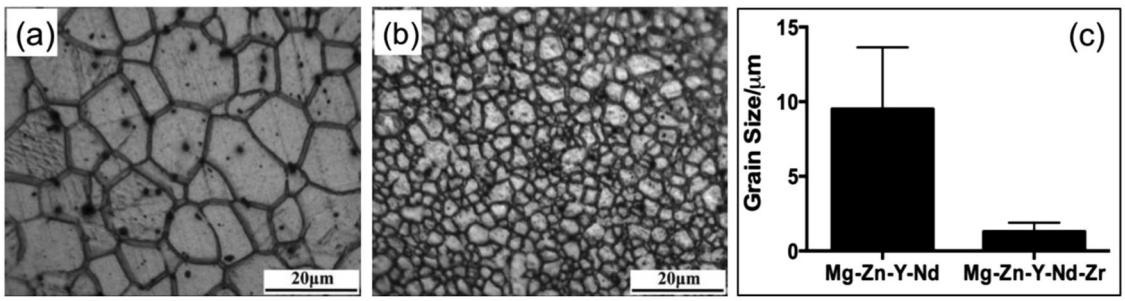

Fig. 1 Microstructure analysis of **a** Mg-Zn-Y-Nd, **b** Mg-Zn-Y-Nd-Zr alloys and **c** average grain size of two types of samples

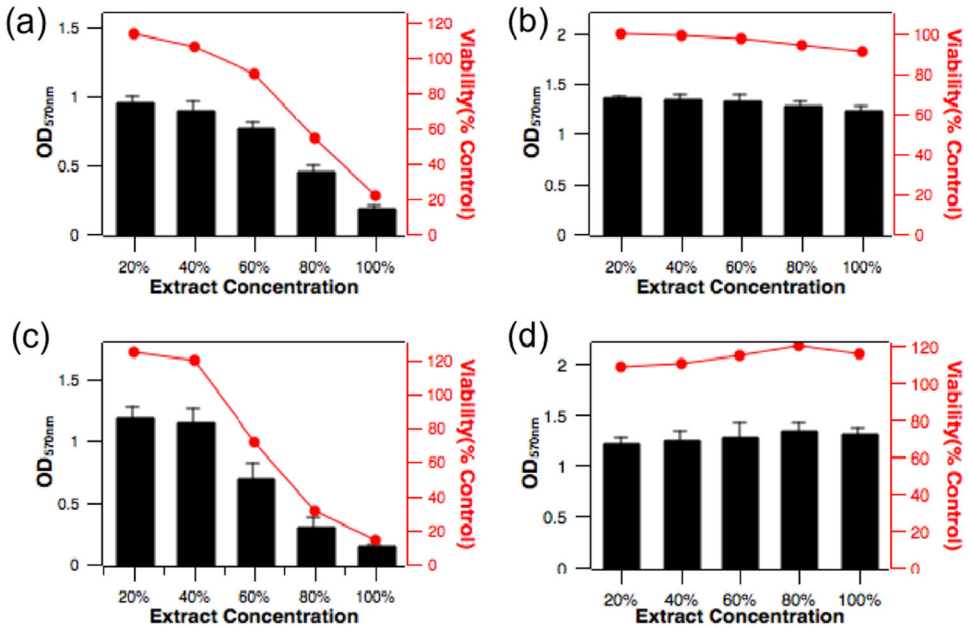

Fig. 3 Cell viability of L929 cultured in Mg-Zn-Y-Nd-Zr extracts prepared for 48 h (**a**, **c**) and 72 h (**c**, **d**). Extracts without pH adjustment (pH≈9.5) (**a**, **c**) and with pH adjustment to 7.4 (**b**, **d**)

Mg-Zn-Y-Nd groups enlarged as the extract concentration increased from 20 to 100% when culturing with either MC3T3-E1 or L929 cells. Interestingly, MC3T3-E1 cells exhibited less sensitivity to the ionic concentration as well as composition of extracts as compared to L929 cells.

3.3 Long-term cytotoxicity analysis

With advancement in grain refinement, the corrosion resistance of Mg-Zn-Y-Nd-Zr alloys has been improved, and a good cytotoxicity result for 24 h was obtained with the viability over 100% for both L929 and MC3T3-E1cells. However, the available standard for *in vitro* cytotoxicity test (ISO 10993-5/12) was designed without considering the generation and accumulation of degradation products during the extract preparation process. Therefore, to evaluate the accumulation effect of released ions from Mg-Zn-Y-Nd-Zr samples, the immersion period for extract preparation was prolonged to 48, 72, 120, 240 and 1440 h.

3.3.1 Influence of high pH values on L929 and MC3T3-E1 cell viability

Figures 3 and 4 demonstrated the viability results of L929 and MC3T3-E1 cells culturing with Mg-Zn-Y-Nd-Zr extracts for 48 and 72 h, respectively. The pH value of extracts was measured to be approximately 9.5, and for comparison purpose, it was then adjusted to 7.4 with 1 M HCl. As for L929 cells, it can be observed that the survival rates decreased with the increase of extract concentrations for both 48 and 72 h. In addition, both 100% extracts exhibited severe cytotoxicity, which was not agreed with the cytotoxicity result for 24 h. However, the viability maintained steadily above 90% for all of the extract concentrations, when the pH was adjusted to 7.4, indicating the good cytocompatibility (as shown in Fig. 3b, d). Furthermore, the absolute values of viability of all the concentrations in 72h-immersion group slightly increased higher than that of 48h-immersion group correspondingly, indicating faster cellular metabolism. As for MC3T3-E1 cells, there were no significantly differences of viability after adjusting the pH value to be neutral, and acceptable cytocompatibility with the viability over 90% was obtained for all the extracts in both 48h-immersion and 72h-immersion groups. In addition, the variations of the viability among extracts of all the concentrations were unremarkable.

3.3.2 Influence of accumulated metallic ions on L929 and MC3T3-E1 cell viability

To investigate the influence of accumulated metallic ions on cytotoxicity, Mg-Zn-Y-Nd-Zr extracts were collected at the time point of 24, 48, 72, 120, 240 and 1440 h, followed by the pH adjustment to 7.4, of which the MTT results had been demonstrated in Figs. 5–7. It can be observed in Figs. 5 and 7 that no cytotoxicity was observed in all the concentrations of extracts collected at the time point of 24, 48, 72, 120 and 240 h for both two cell types. However, when extending to 1440 h, severe cytotoxicity turned up (demonstrated in Figs. 6 and 8). By continuously diluting the extracts, the toxic concentrations of Mg-Zn-Y-Nd-Zr extracts were limited to within 10% for both two cell types. Furthermore, there was selective cellular response of Mg-Zn-Y-Nd-Zr extracts to L929 and MC3T3-E1 cells. When

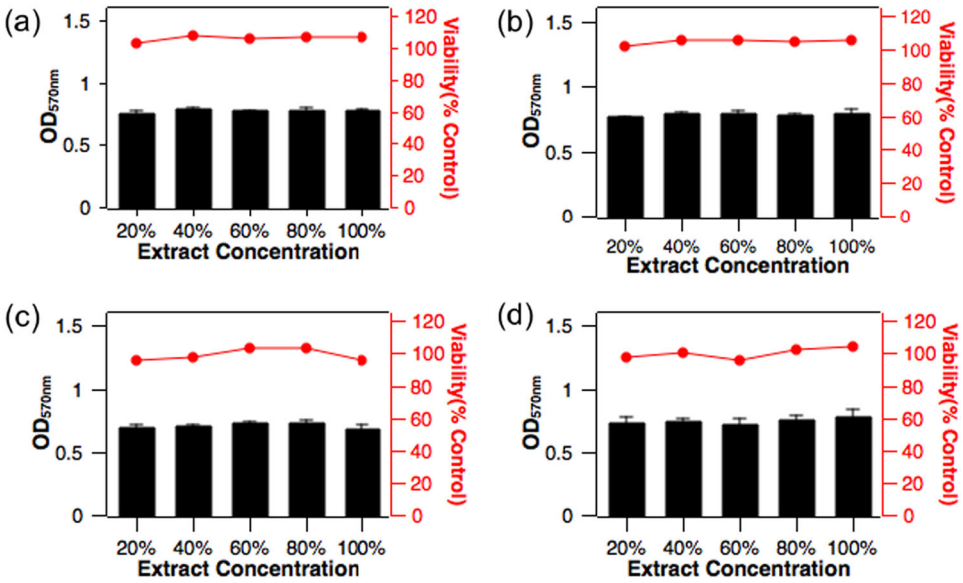

Fig. 4 Cell viability of MC3T3-E1 cultured in Mg-Zn-Y-Nd-Zr extracts prepared for 48 h (**a**, **c**) and 72 h (**c**, **d**). Extracts without pH adjustment (pH≈9.5) (**a**, **c**) and with pH adjustment to 7.4 (**b**, **d**)

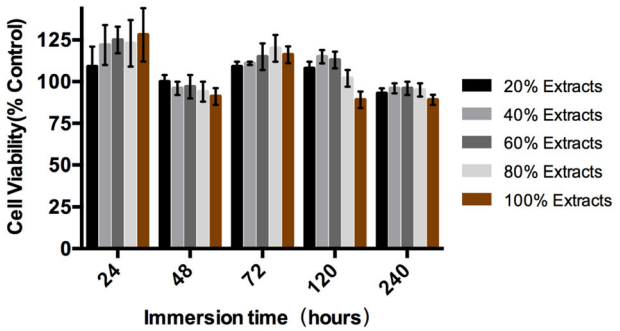

Fig. 5 L929 viabilities cultured in Mg-Zn-Y-Nd-Zr extracts prepared for up to 240 h. All solutions were adjusted to pH = 7.4 with 1 M HCl

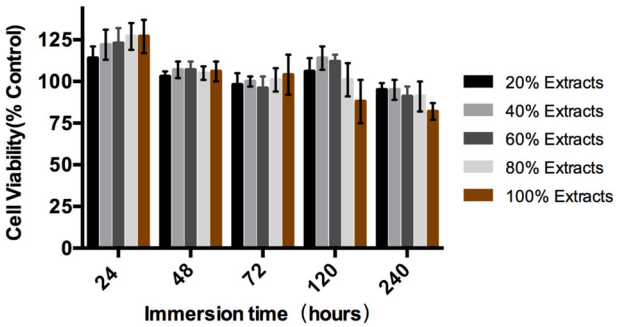

Fig. 7 MC3T3-E1 cultured in Mg-Zn-Y-Nd-Zr extracts prepared for up to 240 h. All the solutions were adjusted to pH = 7.4 with 1 M HCl

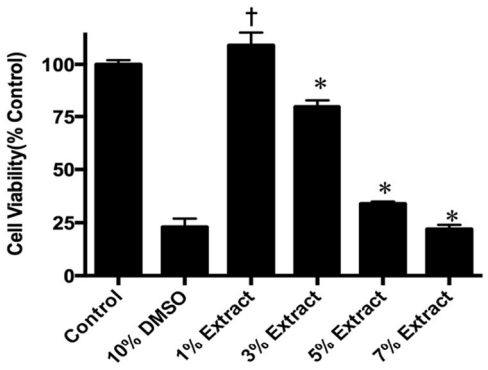

Fig. 6 L929 viabilities cultured in Mg-Zn-Y-Nd-Zr extracts prepared for 1440 h. All the solutions were adjusted to pH = 7.4 with 1 M HCl. *$p < 0.001$ and †$p < 0.05$ compared to the control group

the survival rates of L929 were lower than 75%, the extract concentrations ranged within 3–5%; comparatively, the toxic extract concentrations to MC3T3-E1 were within 5–7%.

To further investigate the cytotoxic effect of Mg-Zn-Y-Nd-Zr extracts, cell morphology was recorded during the cultivation and then demonstrated in Fig. 9. Normal L929 cells exhibited spindle shape with clear cellular outlines, such as cells in control group; on the contrary, cells in 10% DMSO group transformed into irregular circular shape with ambiguous outlines and incomplete membrane, indicating severe cytotoxicity. When the extract concentration increased to 7%, cell number decreased and simultaneously shape evolution occurred, implying the depressed cell metabolism as well as cellular dysfunction. In accordance with the result shown in Fig. 7, abnormal cell morphology was only observed when the extract concentration was lower than 3%.

To identify the cytotoxic level of metallic ions in extracts, Table 2 summarized the amount of the induced ions including Mg^{2+}, Zn^{2+}, Y^{3+}, Nd^{3+} and Zr^{4+} at all the time points. In consideration of cell survival rate demonstrated in Fig. 6 and Fig. 8, the accumulated amount of metallic ions leading to severe cytotoxicity (survival rate < 75%) were measured and then calculated to be 948–1580 μg/ml of Mg^{2+}, 0.2304–0.384 μg/ml of Zn^{2+}, 0.0395–0.0658 μg/ml of Y^{3+}, 0.0448–0.0747 μg/ml of

Table 2 Concentrations of the accumulated Mg^{2+}, Zn^{2+}, Y^{3+}, Nd^{3+} and Zr^{4+} ions in Mg-Zn-Y-Nd-Zr extracts collected at 24, 48, 72, 120, 240 and 1440 h

Immersion time (h)	Ion concentrations (μg/ml)				
	Mg2+	Zn2+	Y3+	Nd3+	Zr4+
24	171.2	0.434	0.1056	0.1948	0.015
48	260	0.834	0.226	0.326	0.0422
72	546	1.238	0.232	0.364	0.0858
120	592	1.545	0.244	0.412	0.0854
240	680	2.08	0.454	0.454	0.1084
1440	31600	7.68	1.316	1.494	0.328

Nd^{3+}, 0.0098–0.0164 μg/ml of Zr^{4+} for L929 cells, and 1580–2212 μg/ml of Mg^{2+}, 0.384–0.538 μg/ml of Zn^{2+}, 0.0658–0.0921 μg/ml of Y^{3+}, 0.0747–0.105 μg/ml of Nd^{3+}, 0.0164–0.0230 μg/ml of Zr^{4+} for MC3T3-E1 cells.

3.4 Cell adhesion

Good initial cell adhesion could ensure the subsequent cell spreading and proliferation. Figures 10 and 11 exhibited the exfoliated cells from surface of samples as shown in the white shear and cells were in spherical shape as a result of trypsinization. Few cells were digested from the surface of Mg-Zn-Y-Nd samples whereas massive spherical L929 and MC3T3-E1 cells were observed around Mg-Zn-Y-Nd-Zr samples. The calculated cell adhesion rates were shown in Figs. 10c and 11c. While L929 and MC3T3-E1 were barely adhere on the surface of Mg-Zn-Y-Nd alloy, they could adhere on the surface of Mg-Zn-Y-Nd-Zr alloy at adhesion rates of 41% for MC3T3-E1 and 28% for L929, indicating improved cytocompatibility compared to Mg-Zn-Y-Nd under direct contact.

3.5 Cell differentiation

3.5.1 ALP activity

The synthesis and secretion of ALP represents earlier maturation of osteoblast differentiation, indicating good functionality. ALP can promote hydrolysis of organic phosphate compounds in the matrix, such as *β*-glycerophosphate (β-GP), to inorganic phosphate ions which combine to Ca^{2+}, forming hydroxyapatite [18]. As shown in Fig. 12, the ALP activity was significantly increased during the differentiation process of osteoblasts from BMSCs induced by the extracts of Mg-Zn-Y-Nd-Zr compared with control group (osteogenic medium). In comparison with the control group, the ALP activity of 25% Mg-Zn-Y-Nd-Zr group increased by about 40%. With the ascending concentrations of alloy extracts, ALP activity of Mg-Zn-Y-Nd-Zr decreased slightly, but the absorbance value of 100% Mg-Zn-Y-Nd-Zr group was still significantly higher than the control group.

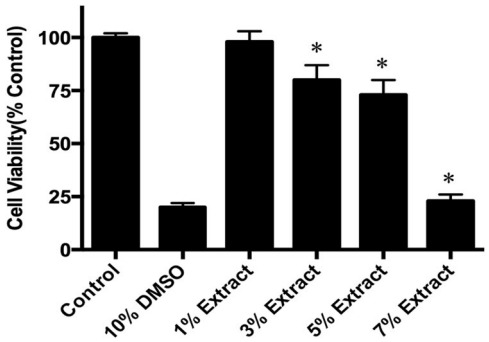

Fig. 8 MC3T3-E1 viabilities cultured in Mg-Zn-Y-Nd-Zr extracts prepared for 1440 h. All the solutions were adjusted to pH = 7.4 with 1 M HCl. *$p < 0.001$ compared to the control group

3.5.2 Alizarin red staining

Calcified nodules are the latter expression of osteogenic phenotype of osteoblasts *in vitro* cultivation [18]. As shown in Fig. 13a, red granular precipitates were observed in the both groups under inverted phase contrast microscope (Nikon Eclipss Ts100, Japan). To quantify the calcification, the number of calcified nodules was measured and demonstrated in Fig. 13b. The formation of calcified nodules in extracts was higher than control group, indicating that Mg-Zn-Y-Nd-Zr significantly promoted the osteogenic differentiation process of BMSCs and the promoting efficacy to bone differentiation should be contributed to the degraded ions of Mg^{2+}, Zn^{2+}, Y^{3+}, Nd^{3+}, Zr^{4+}, which was consistent with the results of ALP activity.

4 Discussion

This study aimed to investigate the cytocompatibility of a novel Mg-Zn-Y-Nd-Zr alloy for bone implant application through *in vitro* cell study.

4.1 Mg-Zn-Y-Nd-Zr exhibited no cytotoxicity

Mg-Zn-Y-Nd-Zr alloy showed no toxicity to L929 and MC3T3-E1cells owing to its excellent corrosion resistance in comparison with Mg-Zn-Y-Nd. Since the cytotoxicity test utilized the indirect extract method, electrochemical reactions must be considered when magnesium alloys were placed in the corrosive medium containing Cl^-, and the equations were as follows:

$$Mg \rightarrow Mg^{2+} + 2e \quad (1)$$

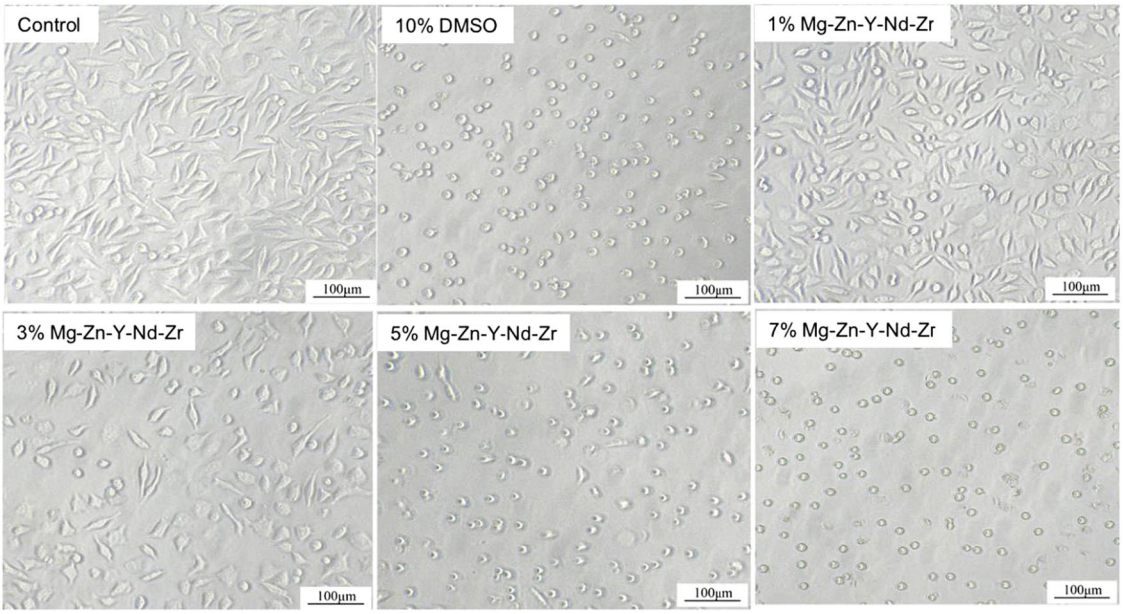

Fig. 9 L929 morphologies cultured in Mg-Zn-Y-Nd-Zr extracts for 1440 h. The solution was adjusted to pH = 7.4 with 1 M HCl

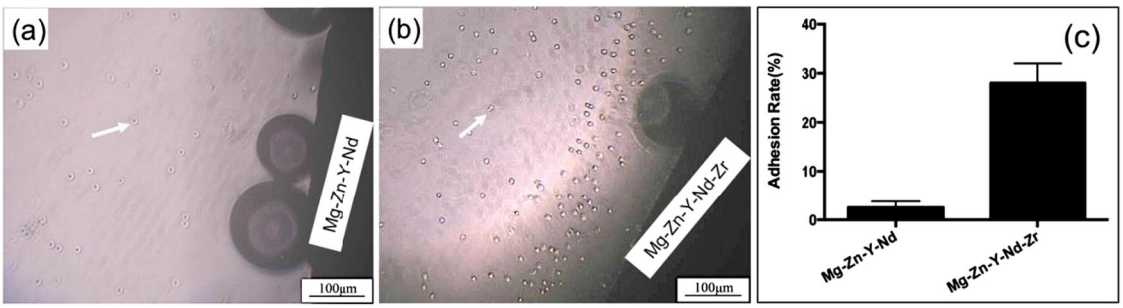

Fig. 10 Exfoliated L929 cells from surface of **a** Mg-Zn-Y-Nd and **b** Mg-Zn-Y-Nd-Zr

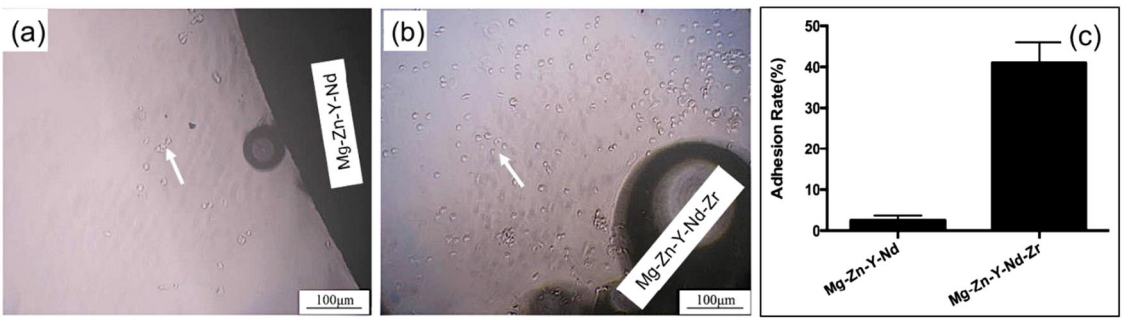

Fig. 11 Exfoliated MC3T3-E1 cells from surface of **a** Mg-Zn-Y-Nd and **b** Mg-Zn-Y-Nd-Zr

$$2H_2O + 2e \rightarrow H_2 + 2OH^- \quad (2)$$

$$Mg^{2+} + OH^- \rightarrow Mg(OH)_2 \quad (3)$$

$$Mg(OH)_2 + 2Cl^- \rightarrow MgCl_2 + 2OH^- \quad (4)$$

During the degradation process, cell culture medium changed in three aspects: alkalization of medium, ascending Mg and alloying ion concentrations, and higher osmotic pressure induced by higher ion concentrations [19]. All the changes may lead to cell apoptosis, and the alteration of medium microenvironment in terms of physical and chemical properties highly depends on the alloys' degradation

rate in medium. Therefore, different cytotoxicity results were obtained for Mg-Zn-Y-Nd and Mg-Zn-Y-Nd-Zr alloys, which illustrated that. The degradation rate indeed played a dominant role in determining cell survival. To be specific, grain sizes of Mg-Zn-Y-Nd-Zr alloys reduced due to the addition of Zr as compared to Mg-Zn-Y-Nd, resulting in more uniform microstructure and higher corrosion resistance (as shown in Figs. 1 and 2). On the other hand, pH value of Mg-Zn-Y-Nd extracts increased rapidly after the 24-h immersion in the cell culture medium due to the rapid corrosion as compared to Mg-Zn-Y-Nd-Zr extracts, and the amount of Mg, Zn as well as rare earth elements in the solution increased quickly, all of which eventually led to the serious cell death.

4.2 Long-term cytotoxicity analysis

Magnesium-based alloys are biodegradable and this type of metallic material possesses unique physiochemical properties when serves in biological environment. Generally, Mg-based metallic materials will react with water immediately and release various kinds of metallic ions accompanied with higher pH value and osmolality in the surrounding medium [19, 20]. Moreover, it has been reported that the ascent of osmolality may not be a critical parameter influencing cell viability [19]. Hence, there are two main variables (pH values and metallic ions) being discussed as the predominant factors influencing cytotoxicity results (as shown in Fig. 14).

4.2.1 Influence of alkaline environment on cells death co-cultured under short-term immersion solutions

It has been reported that the most favorable pH values for cell growth is suggested between 7.4 and 7.8, and alkalosis and acidosis may inhibit protein synthesis for some cells, ultimately inducing cell apoptosis [20]. As shown in Fig. 3, when the extract concentrations (pH ≈ 9.5) increased, survival rates of L929 showed a significant downward trend. However, after the pH values were adjusted to 7.4, the cell viability regained. In addition, there were no remarkable differences in viability between groups. This sharp contrast indicated that the high pH value was the primary factor to L929 cell apoptosis after the 48-hour and 72-hour degradation. Meanwhile, the released metallic ions did not cause severe cell apoptosis of L929 after short-term immersion. According to Fig. 4, MC3T3-E1 cells were cultured in extracts collected from 48-h and 72-h immersion, and no cytotoxicity was observed. The released metallic ions accompanied by Mg-Zn-Y-Nd-Zr short-term degradation were also non-toxic to MC3T3-E1. After the adjustment of

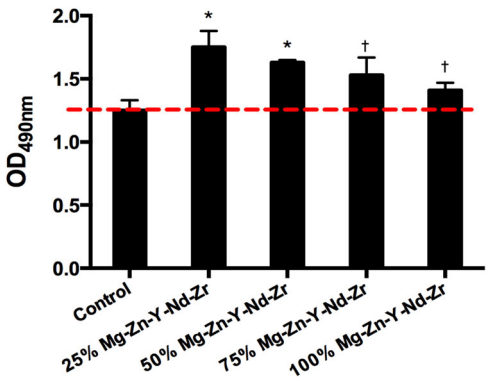

Fig. 12 Enzymatic activity of intracellular ALP cultured in Mg-Zn-Y-Nd-Zr extracts measured at 490 nm. *$p < 0.001$ and †$p < 0.05$ compared to the control group

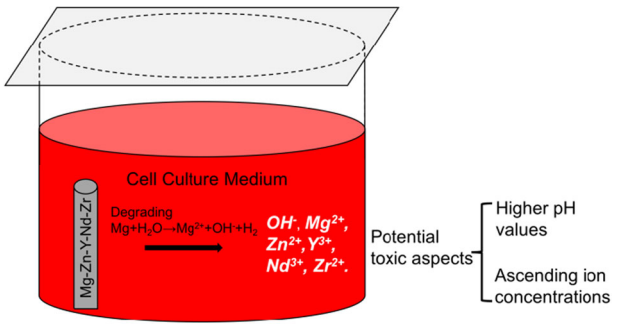

Fig. 14 Diagram of the degradation effects of Mg-Zn-Y-Nd-Zr alloy on the surrounding cell culture medium

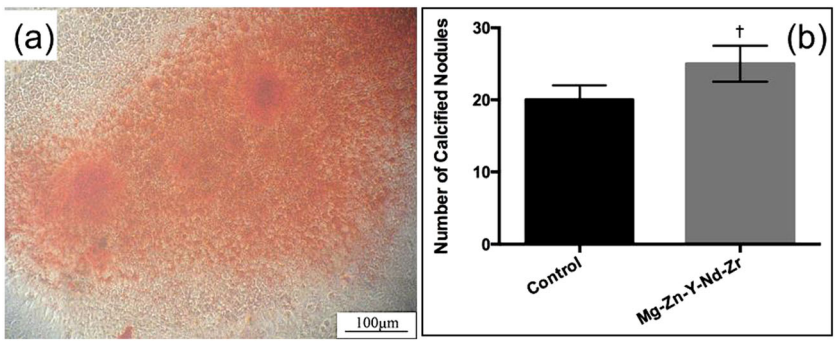

Fig. 13 Calcified nodules stained by Alizarin red in osteoblasts differentiating from BMSCs. **a** Morphology under inverted phase contrast microscope and **b** calcified nodule counting in different osteogenic groups. †$p < 0.05$ compared to the control group

pH value to 7.4, the cell viability did not change remarkably. This inapparent difference implied that MC3T3-E1 cells were more adaptable to alkaline environment in comparison with L929. The main reason of different toxic phenomena of short-term Mg-Zn-Y-Nd-Zr immersion solutions in the case of L929 and MC3T3-E1 may be that L929 and MC3T3-E1 showed different tolerance to alkaline environment. These results support Wang's [19] findings, which showed as pH of the surrounding media was higher than 8.5, survival rate of L929 cells would be about 10% decrease, whereas that of MC3T3-E1 increased slightly. Hence, alkaline environment causes L929 cells death under short-term immersion solutions instead of released metallic ions. Also we suggest tolerance of different cell types to alkaline environment should be taken into consideration in further cytotoxicity experiment design of degradable magnesium-based orthopaedic implants.

In vitro experiments demonstrated the potential hazards of alkalosis. However, according to the previous studies, higher pH around the implants has not been considered to be the main reason limiting their clinically application [1, 2]. Due to the functional $HCO_3^{2-}/H_2CO_3^-$ buffer system and the circulation effect, the pH value of normal human plasma is expected to remains stable at 7.4 after implanting Mg-Zn-Y-Nd-Zr alloy *in vivo*.

4.2.2 Highly concentrated metal ions resulted in cells death co-cultured under long-term immersion solutions

The local bony environment of orthopaedic implant makes it possible for accumulation of metallic ions [21]. Researchers have proved the accumulation of Gd in the animal organs [22]. Liu [23] studied distribution and accumulation of Nd in body of mice using radioisotope tracer method and proved its accumulation in bone was high and increased in amount with time. Therefore, it is crucial to consider the effect of localized ions, especially the rare earth elements on the cytotoxicity. To further analyze the potential hazard during alloy degradation, a series of greater concentrations of ions were obtained by extending the immersion time to make more metallic ions dissolve in the cell culture medium during degradation process and then cytotoxicity of accumulated metal ions on L929 and MC3T3-E1 were analyzed through MTT assay. The pH value was adjusted to 7.4 for clarification. Varied toxic metallic ion concentrations were obtained according to adopted cell types, specifically, 39.5–65.8 μM of Mg^{2+}, 3.5–5.9 μM of Zn^{2+}, 0.44–0.74 μM of Y^{3+}, 0.3–0.52 μM of Nd^{3+}, 0.11–0.18 μM of Zr^{4+} for L929, and 65.8–92.2 μM of Mg^{2+}, 5.9–8.3 μM of Zn^{2+}, 0.74–1.04 μM of Y^{3+}, 0.52–0.73 μM of Nd^{3+}, 0.18–0.25 μM of Zr^{4+} for MC3T3-E1 cells. Similar phenomena have been observed in previous studies. Feyerabend [21] explored different sensitivity of MG63, HUCPV and RAW 264.7 towards metallic elements including Y, Nd, Dy, Pr, Gd, La, Ce, Eu, Li, Zr, Mg and Ca in chloride solution. For MG63, LD_{50} were determined when 50 mM Mg was added; for HUCPV, 80 mM Mg; for RAW 264.7, 50-60 mM Mg. Statistical analysis showed that for RAW 264.7, compared with the control group, the concentration of Y was 200 M when significant viability drop was observed and the corresponding Nd concentration was 700 M. For HUCPV cells, the concentrations were 2000 M for Y, 2000 M for Nd. Feyerabend [21] pointed out that RAW 264.7 showed a very sensitive response to the variation of magnesium and calcium ion concentrations, and survival rate of HUCPV cells was relatively slowly decreased with the increase of Mg^{2+} and Ca^{2+} concentrations. Rim [24] reviewed that LC_{50} of neodymium oxide was 101 μM in an *in vitro* cytotoxicity assay system using rat pulmonary alveolar. However, dissimilarly, Mg^{2+}, Zn^{2+}, Y^{3+}, Nd^{3+} and Zr^{4+} ions concentrations resulting in survival rates of L929 and MC3T3-E1 lower than 75% were far below the toxic concentrations observed in the above experiments in which a single element was evaluated the cytotoxicity. For this, the possible reasons for the selective cellular response can be concluded as that except for adoption of different cell types, there might be intracellular interactions between the different metallic ions. Thus, toxic effect of mixed metallic ions to cells increased in comparison with that of one single element and eventually leaded to cell apoptosis at a relatively lower concentration. However, further exploration and experiments *in vivo* is needed to prove this hypothesis.

4.3 Released metallic ions helped to promote osteogenic differentiation process during Mg-Zn-Y-Nd-Zr degradation

Cell differentiation experiments showed that Mg-Zn-Y-Nd-Zr alloy obviously promoted the osteogenic differentiation process. Since the pH value had been adjusted to 7.4 to avoid the negative cellular effect, the concentration and combination of metallic ions in extracts might be attributed to the differentiation results.

Mg exists in the human body, in which about 67% exists in bone tissue [25]. The results of *in vivo* implantation of magnesium alloys in early time showed that the magnesium ions had the osteogenic properties, which could stimulate the formation of new bone after implantation [26, 27]. Zn is also an essential trace element in human body. Some scholars believed that Zn could promote adhesion process of osteoblast cells *in vitro* and the expression of osteogenic-related genes [28, 29]. On the other hand, lanthanide rare earth elements and calcium ions have a lot of common properties, such as similar ionic radius, the same number of outer electrons, as shown in Table 3. Studies [30] have

Table 3 Comparison of ionic radius of Ca, Y and Nd

Ion	Ca^{2+}	Y^{3+}	Nd^{3+}
Ionic radius	0.99Å	0.89 Å	0.995 Å
Outer electron	3p6	4p6	4f3

proved rare earth elements could replace Ca^{2+} in cell membrane enzyme protein and impact influx of Ca^{2+}; Similarly, Zhang [11] found that the Y element promoted the formation of calcified matrix of osteoblasts at 10^{-4} and 10^{-5} mol/L; and feeding experiments on ovariectomized mice found that rare earth elements inhibited bone resorption and stimulated osteoblast activity, thus increasing bone density in mice. In addition, it was found that the addition of rare earth oxide additives promoted the osteogenic differentiation of human bone marrow mesenchymal stem cells and the accumulation of collagen in *in vitro* studies. As the grain refiner in alloys, there are some controversies about the biocompatibility of Zr. Saha [3] showed that the grain of the alloys was refined by the addition of Zr element, and the refined grains of magnesium alloy severely restricted the differentiation of osteoclast. Comparatively, Depprich [30] evaluated the biocompatibility of titanium alloy and structured zirconia using primary bovine osteoblastic cells. After co-culture of 1, 3, and 5 days with the alloys, cell proliferation was significantly improved on the surface of zirconia. Lee [31] pointed out that Zr element could promote the proliferation of osteoblasts at a low concentration, and inhibit the process at a high concentration in the analysis of the biological potential of Zr. In this study, ALP activity decreased in high concentrations of Mg-Zn-Y-Nd-Zr extracts during osteogenic differentiation, which could be illustrated that high Zr ion concentrations slightly induced the inhibitory effect to the differentiation of osteoblasts. However, the interaction of released Mg^{2+}, Zn^{2+}, Y^{3+}, Nd^{3+}, Zr^{4+} during the degradation process of Mg-Zn-Y-Nd-Zr alloys generally promoted the differentiation induction of BMSCs into osteoblasts.

5 Conclusions

In this study, cytocompatibility of Mg-Zn-Y-Nd-Zr alloy was theoretically evaluated and analyzed by *in vitro* cell test followed by the ISO 10993 standard, of which the result indicated non-cytotoxicity of Mg-Zn-Y-Nd-Zr alloy to L929 and MC3T3-E1 cells. Both types of cells can adhere and well spread in extracts. In addition, high expression of ALP activity and calcified nodules implied that alloying elements can promote the osteogenic differentiation. This study first proposes the Mg-Zn-Y-Nd-Zr alloy as the potential candidate for orthopedic application with improved corrosion resistance, non-cytotoxicity as well as osteogenic properties; and when taking possibility of the metallic ion accumulation in bone into consideration, the cytotoxic levels of accumulated ion concentrations (Mg^{2+}, Zn^{2+}, Y^{3+}, Nd^{3+}, Zr^{4+}) have been revealed to be 39.5–65.8 μM of Mg^{2+}, 3.5–5.9 μM of Zn^{2+}, 0.44–0.74 μM of Y^{3+}, 0.3–0.52 μM of Nd^{3+}, 0.11–0.18 μM of Zr^{4+} for L929, and 65.8–92.2 μM of Mg^{2+}, 5.9–8.3 μM of Zn^{2+}, 0.74–1.04 μM of Y^{3+}, 0.52–0.73 μM of Nd^{3+}, 0.18–0.25 μM of Zr^{4+} for MC3T3-E1 cells. Although experiments *in vivo* are needed in future to further prove the functionality of Mg-Zn-Y-Nd-Zr alloys serving as orthopaedic implants, this study can still remarkably guide the biodegradable magnesium-based alloy design and provide scientific evidence for clinical practice.

Acknowledgements SKG and XZS are supported by the National High-tech Research and Development Projects (863) (Grant No.2015AA033603; No.2015AA020301), National Key Research and Development Program of China (Grant No. 2016YFC1102403) and the Major Science and Technology Projects in Henan Province (141100310900). LC is supported by National Natural Science Foundation of China (Grant No. 51601169).

Compliance with ethical standards

Conflict of interest The authors declare that they have no conflict of interest.

References

1. Staiger MP, Pietak AM, Huadmai J, et al. Magnesium and its alloys as orthopedic biomaterials: A review. Biomaterials. 2006;27:1728–34.
2. Zheng YF, Gu XN, Witte F. Biodegradable metals. Mater Sci Eng R. 2014;77:1–34.
3. Saha P, Roy M, Datta MK, et al. Effects of grain refinement on the biocorrosion and in vitro bioactivity of magnesium. Mater Sci & Eng C. 2015;57:294–303.
4. TSNS Narayanan, Park, Min IS, Strategies HL. to improve the corrosion resistance of microarc oxidation (MAO) coated magnesium alloys for degradable implants: prospects and challenges. Prog Mater Sci. 2014;60:1–71.
5. Rosalbino F, De NS, Scavino G, et al. Microstructure and in vitro degradation performance of Mg-Zn-Mn alloys for biomedical application. J Biomed Mater Res A. 2013;101:704–11.
6. Tie D, Guan R, Liu H, et al. An in vivo study on the metabolism and osteogenic activity of bioabsorbable Mg-1Sr alloy. Acta Biomater. 2015;29:455–67.
7. Chou DT, Hong D, Saha P, et al. In vitro and in vivo corrosion, cytocompatibility and mechanical properties of biodegradable Mg-Y-Ca-Zr alloys as implant materials. Acta Biomater. 2013;9:8518–33.
8. Sansone V, Pagani D, Melato M. The effects on bone cells of metal ions released from orthopaedic implants. A review. Clin Cases Mineral Bone Metabolism. 2013;10:34–40.
9. Wang B, Guan S, Wang J, et al. Effects of Nd on microstructures and properties of extruded Mg–2Zn–0.46Y– x Nd alloys for stent application. Mater Sci Eng B. 2011;176:1673–8.

10. Willbold E, Gu X, Albert D, et al. Effect of the addition of low rare earth elements (lanthanum, neodymium, cerium) on the biodegradation and biocompatibility of magnesium. Acta Biomater. 2015;11:554–62.
11. Zhang JC, Liu CL, Li YP, et al. Effect of yttrium ion on the proliferation, differentiation and mineralization function of primary mouse osteoblasts in vitro. J Rare Earths. 2010;28:466–70.
12. Salem R, Hunter RD. Yttrium-90 microspheres for the treatment of hepatocellular carcinoma: a review. Int J Radiat Oncol Biol Phys. 2006;127:S194–205.
13. Kokubo T, Takadama H. How useful is SBF in predicting in vivo bone bioactivity? Biomaterials. 2006;27:2907–15.
14. ISO 10993-12: biological evaluation of medical devices: Sample preparation and reference materials. International Organization for Standardization. 2004; 1–8.
15. ISO 10993-5: biological evaluation of medical devices: Tests for in vitro cytotoxicity. International Organization for Standards. 2009; 1–11.
16. Zhai YK, Pan YL, Niu YB, et al. The importance of the prenyl group in the activities of osthole in enhancing bone formation and inhibiting bone resorption in vitro. Int J Endocrinol. 2014;9: 921–54.
17. Alvarez-Lopez M, Pereda MD, Valle JAD, et al. Corrosion behaviour of AZ31 magnesium alloy with different grain sizes in simulated biological fluids. Acta Biomater. 2010;6:1763–71.
18. Beck GR. Inorganic phosphate as a signaling molecule in osteoblast differentiation. J Cell Biochem. 2003;90:234–43.
19. Wang J, Witte F, Xi T, et al. Recommendation for modifying current cytotoxicity testing standards for biodegradable magnesium-based materials. Acta Biomater. 2015;21:237–49.
20. Cutaia M, Black AD, Cohen I, et al. Alkaline stress-induced apoptosis in human pulmonary artery endothelial cells. Apoptosis. 2005;10:1457–67.
21. Feyerabend F, Fischer J, Holtz J, et al. Evaluation of short-term effects of rare earth and other elements used in magnesium alloys on primary cells and cell lines. Acta Biomater. 2010;6:1834–42.
22. Myrissa A, Braeuer S, Martinelli E, et al. Gadolinium accumulation in organs of Sprague-Dawley (®) rats after implantation of a biodegradable magnesium-gadolinium alloy. Acta Biomater. 2017;48:521–9.
23. Liu Y, Chen Z, Wang Y. Distribution and accumulation of neodymium in body of mice and effect on progesterone secretion. J Chinese Rare Earth Soc. 2001;19:447–9.
24. Rim KT, Koo KH, Park JS. Toxicological evaluations of rare earths and their health impacts to workers: a literature review. Saf Health Work. 2013;4:12–26.
25. Okuma T. Magnesium and bone strength. Nutrition. 2001;17:679–80.
26. Gao JH, Shi XY, Yang B, et al. Fabrication and characterization of bioactive composite coatings on Mg-Zn-Ca alloy by MAO/sol-gel. J Mater Sci: Mater Med. 2011;22:1681–7.
27. Han P, Cheng P, Zhang S, et al. In vitro and in vivo studies on the degradation of high-purity Mg (99.99wt.%) screw with femoral intracondylar fractured rabbit model. Biomaterials. 2015;64: 57–69.
28. Ikeuchi M, Ito A, Dohi Y, et al. Osteogenic differentiation of cultured rat and human bone marrow cells on the surface of zinc-releasing calcium phosphate ceramics. J Biomed Mater Res A. 2003;67:1115–22.
29. Ito A, Ojima K, Naito H, et al. Preparation, solubility, and cytocompatibility of zinc-releasing calcium phosphate ceramics. J Biomed Mater Res A. 2000;50:178–83.
30. Depprich R, Ommerborn M, Zipprich H, et al. Behavior of osteoblastic cells cultured on titanium and structured zirconia surfaces. Head Face Med. 2008;4:29–39.
31. Lee DB, Roberts M, Bluchel CG, et al. Zirconium: biomedical and nephrological applications. Asaio Journal. 2010;56:550–6.